

Masculine Epigenetic Sex Marks of the CYP19A1/Aromatase Promoter in Genetically Male Chicken Embryonic Gonads Are Resistant to Estrogen-Induced Phenotypic Sex Conversion 1

Authors: Ellis, Haley L., Shioda, Keiko, Rosenthal, Noël F., Coser, Kathryn R., and Shioda, Toshi

Source: *Biology of Reproduction*, 87(1)

Published By: Society for the Study of Reproduction

URL: <https://doi.org/10.1095/biolreprod.112.099747>

The BioOne Digital Library (<https://bioone.org/>) provides worldwide distribution for more than 580 journals and eBooks from BioOne's community of over 150 nonprofit societies, research institutions, and university presses in the biological, ecological, and environmental sciences. The BioOne Digital Library encompasses the flagship aggregation BioOne Complete (<https://bioone.org/subscribe>), the BioOne Complete Archive (<https://bioone.org/archive>), and the BioOne eBooks program offerings ESA eBook Collection (<https://bioone.org/esa-ebooks>) and CSIRO Publishing BioSelect Collection (<https://bioone.org/csiro-ebooks>).

Your use of this PDF, the BioOne Digital Library, and all posted and associated content indicates your acceptance of BioOne's Terms of Use, available at www.bioone.org/terms-of-use.

Usage of BioOne Digital Library content is strictly limited to personal, educational, and non-commercial use. Commercial inquiries or rights and permissions requests should be directed to the individual publisher as copyright holder.

BioOne is an innovative nonprofit that sees sustainable scholarly publishing as an inherently collaborative enterprise connecting authors, nonprofit publishers, academic institutions, research libraries, and research funders in the common goal of maximizing access to critical research.

Masculine Epigenetic Sex Marks of the *CYP19A1/Aromatase* Promoter in Genetically Male Chicken Embryonic Gonads Are Resistant to Estrogen-Induced Phenotypic Sex Conversion¹

Haley L. Ellis,³ Keiko Shioda,³ Noël F. Rosenthal,³ Kathryn R. Coser,⁴ and Toshi Shioda²

Molecular Profiling Laboratory, Massachusetts General Hospital Center for Cancer Research and Harvard Medical School, Charlestown, Massachusetts

ABSTRACT

Sex of birds is genetically determined through inheritance of the ZW sex chromosomes (ZZ males and ZW females). Although the mechanisms of avian sex determination remains unknown, the genetic sex is experimentally reversible by in ovo exposure to exogenous estrogens (ZZ-male feminization) or aromatase inhibitors (ZW-female masculinization). Expression of various testis- and ovary-specific marker genes during the normal and reversed gonadal sex differentiation in chicken embryos has been extensively studied, but the roles of sex-specific epigenetic marks in sex differentiation are unknown. In this study, we show that a 170-nt region in the promoter of *CYP19A1/aromatase*, a key gene required for ovarian estrogen biosynthesis and feminization of chicken embryonic gonads, contains highly quantitative, nucleotide base-level epigenetic marks that reflect phenotypic gonadal sex differentiation. We developed a protocol to feminize ZZ-male chicken embryonic gonads in a highly quantitative manner by direct injection of emulsified ethynylestradiol into yolk at various developmental stages. Taking advantage of this experimental sex reversal model, we show that the epigenetic sex marks in the *CYP19A1/aromatase* promoter involving DNA methylation and histone lysine methylation are feminized significantly but only partially in sex-converted gonads even when morphological and transcriptional marks of sex differentiation show complete feminization, being indistinguishable from gonads of normal ZW females. Our study suggests that the epigenetic sex of chicken embryonic gonads is more stable than the morphologically or transcriptionally characterized sex differentiation, suggesting the importance of the nucleotide base-level epigenetic sex in gonadal sex differentiation.

embryo, endocrine disruptors, epigenetics, gene regulation, sex determination

INTRODUCTION

Gonadal sex differentiation in vertebrates is a sequential and highly organized process. Mammalian sex is determined exclusively by genetic information conveyed by the X and Y

sex chromosomes, whose homogametic combination (XX) makes females and heterogametic combination (XY) makes males. In contrast, in birds, heterogametic combination of their two sex chromosomes Z and W (ZW) is associated with females whereas homogametic combination (ZZ) is associated with males [1]. Different from mammals whose sex is strictly determined by their genotype, control of phenotypic gonadal sex differentiation in birds is reversible by exposure to exogenous hormonal agents, resembling the environmentally vulnerable sex differentiation of lower, ectothermic vertebrates such as reptiles or fish [2]. For example, in ovo exposure of ZZ-male chicken embryos to exogenous estrogens or estrogenic endocrine disruptors during their early stages of development causes male-to-female gonadal sex conversion [2–6]. Conversely, exposure of ZW females to aromatase inhibitors such as fadrozole causes complete and permanent gonadal and total-body sex conversion to males [7–10], demonstrating the critical importance of P450-aromatase (AROM) activity in female sex differentiation [1, 2, 11].

Although the genetic sex of chicken is determined at fertilization, sex-determining genes are activated later during embryonic development, inducing testis or ovary from the bipotential, undifferentiated primordial gonad formed from the intermediate mesodermal tissue on the ventromedial surface of the embryonic mesonephroi [2]. By Day 3.5 of the 21-day in ovo development, the primordial gonads consist of an outer epithelial layer (the cortex) and the internal medulla containing cords of somatic cells and loose mesenchymal cells. The onset of gonadal sex differentiation becomes morphologically evident at Day 6.0–6.5. In ZZ-male gonads, the medullary cords thicken and incorporate germ cells to form seminiferous cords while the cortex shrinks. In contrast, in ZW females, the entire right gonad shrinks and the cords of the medulla in the left gonad become vacuolated to form lacunae, whereas somatic and germ cells in the cortex proliferate in the left gonad [2].

In mammals, biosynthesis of sex steroids is initiated in gonads after completion of their sex differentiation, and the process of gonadal sex differentiation itself is essentially resistant to exogenous sex steroids or their inhibitors [1, 2]. In contrast, estrogen synthesis is observed in still undifferentiated primordial gonads of ZW-female chicken embryos at the time of initiation of morphological gonadal sex differentiation, which itself is highly susceptible to hormonal manipulation. The two critical enzymes required for the terminal steps of estrogen biosynthesis—namely, 17 β -hydroxysteroid dehydrogenase (17 β HSD) and AROM—are expressed only in the medullary cords of the ZW-female gonads immediately before the onset of morphological gonadal differentiation (Day 6.0–6.5) [1, 2, 12–14]. Because other enzymes involved in the upstream steps of sex steroid biosynthesis are expressed in the gonadal medulla of both sexes [14], 17 β HSD and AROM are the only components

¹Supported by the NIH National Cancer Institute (NCI) Federal Share/Program Income Grant (R7963) and the Friends of Mels grant to T.S.

²Correspondence: E-mail: tshioda@partners.org

³These authors contributed equally to this study.

⁴Current address: Department of Molecular Biology, Cell Biology and Biochemistry, Brown University.

Received: 9 February 2012.

First decision: 7 March 2012.

Accepted: 10 April 2012.

© 2012 by the Society for the Study of Reproduction, Inc.

This is an Open Access article, freely available through *Biology of Reproduction's* Authors' Choice option.

eISSN: 1529-7268 <http://www.biolreprod.org>

ISSN: 0006-3363

showing sexual dimorphism in the estrogen biosynthesis pathway. Estrogen receptor α is expressed in the gonadal cortex of both sexes prior to sex differentiation, and its expression in male gonads and the right (i.e., shrinking) female gonads is later suppressed [2, 13, 15]. It is well accepted that estrogens synthesized in the medulla of female gonads mediate ovarian gonadal differentiation by supporting development of the gonadal cortex through the activation of estrogen receptor α and that transient expression of estrogen receptor α in undifferentiated ZZ-male embryonic gonads is responsible for sex reversal by exogenous estrogens [2]. Expression of the forkhead transcription factor FOXL2 is temporospatially similar to expression of 17 β HSD and AROM in ZW-female chicken embryonic gonads, and it has been proposed that FOXL2 may be an important upstream regulator of genes encoding these estrogen-synthesizing enzymes [10, 16, 17].

Recent studies revealed critical roles of the Z chromosome-linked *DMRT1* gene and the chicken male hypermethylated region (cMHM) located adjacent to the *DMRT1* locus on the Z chromosome in male sex determination of chicken embryonic gonads [2, 18–20]. It has been proposed that the cMHM is hypermethylated to transcriptionally inactive status in male primordial gonads and that noncoding RNA transcripts expressed exclusively from the cMHM of female primordial gonads suppress expression of *DMRT1*, currently the best candidate master masculinizing gene of chicken gonads. Thus, mechanisms regulating *DMRT1* expression by cMHM suggest the importance of epigenetic regulation of gene expression in the process of gonadal sex differentiation in chicken embryos [2, 19, 21]. However, little information is presently available on epigenetic marks of other, autosomal key genes involved in chicken gonadal sex determination.

In the present study, we identified highly quantitative, phenotypic sex-dependent changes in nucleotide-level epigenetic marks located within a 170-nt region of the promoter of *CYP19A1* gene, which is on the autosomal chromosome 10 and encodes AROM. We also show that these epigenetic sex marks are partially feminized in gonads of ZZ males sex-converted by in ovo exposure to a synthetic estrogen. Interestingly, the epigenetic sex marks still significantly retained a partially masculine profile even in strongly feminized gonads whose morphological and transcriptional markers of sex differentiation are indistinguishable from those of normal ZW-female gonads. Our study provides the first example of highly quantitative, nucleotide base-level epigenetic marks in a promoter of key autosomal gene involved in sex differentiation of chicken embryonic gonads and suggests that the epigenetic sex of gonads may be more resistant to environmentally induced sex reversal than transcriptional or morphological marks of gonadal sex differentiation.

MATERIALS AND METHODS

Egg Incubation, Sex Typing, and Induced Feminization

All the animal experiments were approved by the Institutional Animal Care and Use Committee. Fertile research-grade SPF eggs of White Leghorn chickens (*Gallus gallus domesticus*) were obtained from Charles River Laboratories and incubated under 70%–80% humidity at 37.8°C with intermittent rotations (90° at every 30 min around the horizontally laid long axis of eggs) in a research-grade avian egg incubator. Eggs were candled on Day 3.0 (the day initiating incubation is Day 1), and dead eggs were removed from the experiments before further processing. Greater than 95% of eggs alive on Day 3.0 hatched on Day 21 of incubation.

For genetic sex typing, 10 μ l venous blood samples were collected from Day 17 embryos and subjected to quantitation of Z and W sex chromosomes by TaqMan qPCR as we previously described [22]. Embryos were dissected on Day 19, and the sex-specific gross morphological characteristics of their gonads (as reviewed in [1, 2]) were scored as shown in Figure 1A. For histological

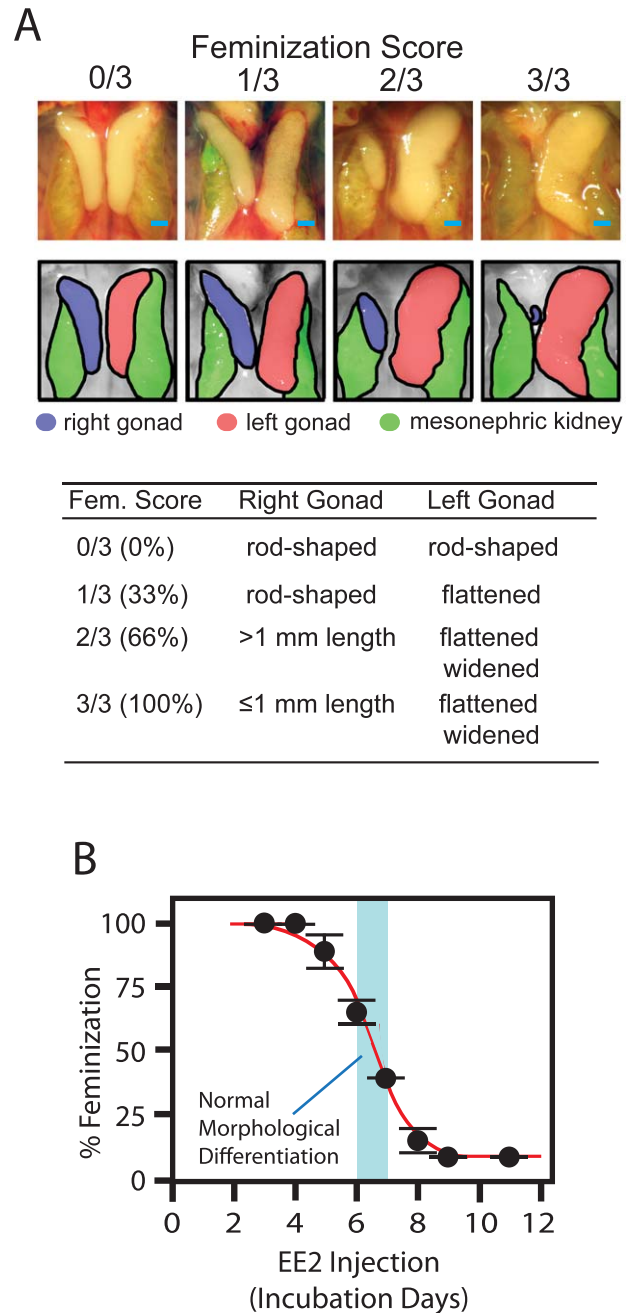


FIG. 1. Feminization of ZZ-male chicken embryonic gonads by exposure to EE2 during early stages of development. **A**) Quantifying the degrees of feminization by gross morphology of Day 19 embryonic gonads. Photographs in the top row show frontal images of ZZ-male embryonic gonads in the retroperitoneal space (bar = 1 mm). Gonads and mesonephric kidneys are identified in the bottom row. Criteria for feminization scoring are shown in the table. **B**) Quantitative gonadal feminization of EE2-exposed ZZ-male gonads depends on the timing of exposure initiation. EE2 exposure (20 μ g/egg) was initiated at the indicated time (x-axis), and its feminization effect was scored (y-axis). Normal morphological differentiation of ZZ testes is observed between Days 6.0 and 7.0 (shown by blue shade). Each datum point indicates mean \pm SEM of averaged feminization scores determined for five different batches of experiments consisting of at least five ZZ-male eggs.

examinations, Day 19 gonadal tissues were fixed with formalin and subjected to hematoxylin and eosin (H&E) staining following a standard protocol. Genomic DNA and total RNA were simultaneously isolated from embryonic gonadal tissues using the AllPrep kit (QIAGEN). The right and left testes of each embryo showed no significant histological differences and were pooled for epigenomic and transcriptomic analyses.

ZZ-male chicken embryos were feminized by injecting emulsion consisting of ethynylestradiol (EE2), peanut oil, lecithin, and water directly into yolk as previously described for experimental sex conversion of Japanese quail embryos [23]. Each egg was injected with 50 μ l emulsion containing 20 μ g EE2 (>98% purity; Spectrum Chemicals) or the same volume of emulsion without EE2 (vehicle control). Upon injection, the oil emulsion containing EE2 immediately surrounded the developing embryos located at the top of yolk because of its buoyancy, ensuring immediate exposure of the embryos to EE2. Emulsion injection into yolk with or without EE2 did not affect viability or overall development of chicken embryos except for sexual differentiation. By our hands, injection of EE2 into albumin or air cell with ethanol, dimethylsulfoxide, or olive oil vehicle resulted in poor reproducibility of experimental feminization, probably because of certain physical unevenness in exposure of embryos to EE2 [24].

Depletion of Gonadal Germline Cells from Somatic Cells by Magnetic-Activated Cell Sorting

Day 19 gonads collected and pooled from 20–40 genotyped embryos were minced by scalpels on ice, digested with trypsin/ethylenediaminetetraacetic acid at 37°C for 30 min, and passed through cell strainers (40 μ m pore size). Single cell suspensions were stained with mouse anti-SSEA-1 (stage-specific embryonic antigen 1) monoclonal antibody (MC-480-c, immunoglobulin M (IgM)- κ light chain; University of Iowa Developmental Studies Hybridoma Bank) and then further stained with fluorescein isothiocyanate (FITC)-conjugated, F(ab')₂ fragment goat anti-mouse IgM μ -chain antibody (Jackson ImmunoResearch). FITC-stained, SSEA-1 positive germline cells were removed from gonadal somatic cells by the magnetic-activated cell sorting (MACS) anti-FITC MicroBeads kit (Miltenyi Biotec). The three-antibody germline cell capture scheme is shown in the supplemental data available online at www.biolreprod.org (see Supplementary Fig. S3A). Two consecutive runs of MACS magnetic purification procedures achieved approximately 70%–80% purity for germline cells and greater than 99.9% purity for gonadal somatic cells, which were confirmed by fluorescence microscopy as shown in the supplemental data (see Supplementary Fig. S3B). Similar MACS-based systems for separating germline cells from gonadal somatic cells have been performed in previous studies for chicken [25–27] and mouse [28]. In our present study, we focus on the germline-depleted somatic cell preparations because of the significant impurity of the MACS-isolated germline cells.

Affymetrix Microarray and Real-Time qPCR

Technical details of Affymetrix microarray and reverse transcription TaqMan qPCR were described in our previous studies [29–31]. Expression of individual mRNA transcripts for gonadal sex marker genes was determined by reverse transcription qPCR TaqMan assays (Applied Biosystems). TaqMan assay identifications (IDs) were as follows: Gg03815934_s1 (ACTB), Gg03346129_g1 (CYP17A1), Gg03366975_m1 (ESR1), Gg03346002_m1 (CYP19A1), and Gg03341744_s1 (FOXL2). Expression of mRNA transcripts for DNA methyltransferases was determined by QuantiTect reverse transcription CYBR Green qPCR assays (QIAGEN) following the manufacturer's protocol. QuantiTect assay IDs were as follows: Gg_GAPDH_1_SG (GAPDH), Gg_DNMT1_1_SG (DNMT1), Gg_DNMT3A_1_SG (DNMT3A), and Gg_DNMT3B_2_SG (DNMT3B).

Bisulfite-Pyrosequencing Determination of CpG Methylation

Purified genomic DNA samples were subjected to bisulfite conversion of unmethylated cytosines to uracils using EZ DNA methylation kit (Zymo Research). Promoter sequences of *CYP19A1* and *ESR1* (identified by boxes in Fig. 4A) were amplified by PCR from bisulfite-converted DNA and subjected to pyrosequencing determination of relative cytosine methylation. Primers for PCR amplification and sequencing are provided as Supplementary Table S1. DNA methylation in the first exon of *DNMT3A* and *DNMT3B* genes was determined by pyrosequencing as previously described [32]. Pyrosequencing reactions and data collection were performed by PyroMark Q96 MD system (QIAGEN).

Chromatin Immunoprecipitation Assay of CYP19A1 Promoter

Chromatin immunoprecipitation (ChIP) assays of chicken embryonic gonads were performed as described in our previous study [33] using the ChIP-IT Express Enzymatic Kit (Active Motif) with modifications. Day 19

gonad(s) isolated from a single embryo was washed with PBS and subjected to crosslinking in 1% formaldehyde freshly diluted in PBS at room temperature for 20 min. Tissue was then washed with PBS and soaked in the crosslinking stop buffer containing a high concentration of glycine provided in the kit at room temperature for 5 min. The fixed tissue was then homogenized in the kit's cell scraping solution on ice using a plastic pestle and a sample cup, and the homogenate was subjected to chromatin isolation, enzymatic fragmentation of chromatin, and immunoprecipitation following the kit's instructions. Immunoprecipitation of the chromatin fragments was performed overnight at 4°C using protein G-conjugated magnetic beads provided in the kit with antibodies to trimethylated H3 histone lysine 4 (H3K4me3), trimethylated H3 histone lysine 27 (H3K27me3), and both the phosphorylated and unphosphorylated forms of the largest subunit of RNA polymerase II (39159, 39156, and 39097, respectively; Active Motif). Magnet-precipitated chromatin was extensively washed, and its DNA-protein crosslinking was reversed by heating at 95°C for 15 min. Chromatin fragments recovered in the supernatant of the heating step were subjected to proteinase K digestion, and a DNA sequence overlapping the differentially methylated CpG sites in chicken *CYP19A1* promoter (as indicated in Fig. 7A) was amplified by PCR using Platinum PCR supermix (Invitrogen) and the following primers: forward, 5'-ACTGCTGCTCCTTTCAGCAT; reverse, 5'-AGGAAGCTTTTGTGGGCT. The 223-nt PCR product was visualized by the FlashGel gel electrophoresis system (Lonza) and quantitated using the ImageJ64 image-processing software (National Institutes of Health).

Statistics

Differences in averages were tested by Student *t*-test (unpaired, two-tail). Heteroscedastic data with significant F-test results ($P < 0.05$) were tested by the Welch *t*-test (unpaired, two-tail).

RESULTS

Quantitative Feminization of ZZ-Male Chicken Embryonic Gonads Induced by Timed Exposure to EE2

Chicken embryos were exposed to a fixed dose of EE2 (20 μ g/egg) emulsified in an oil mixture partly mimicking yolk components [23] and injected directly into yolk at various times during early development. The buoyancy of the emulsion ensured immediate exposure of the embryos to the EE2, which was confirmed by rapid distribution of fluorescein isothiocyanate dye in the entire embryonic tissues observed within minutes after injection (data not shown). Figure 1A shows gross appearance and scoring criteria of morphological feminization applied to normal and feminized ZZ-male gonads observed on Day 19. Exposure of ZZ-male embryos to EE2 initiated on Day 3.0–4.0 resulted in 100% morphological feminization of gonads (i.e., gross appearance of the feminized ZZ gonads was indistinguishable from that of normal ZW-female ovaries) whereas exposure initiated on Day 9.0 had no detectable effects (Fig. 1B). Complete morphological sex reversal of the EE2-exposed ZZ-male gonads was further confirmed by histological examinations, which revealed characteristics of ovarian differentiation, including strong mesenchymal vacuolization and highly thickened cortex containing germ cells [2] (Fig. 2). Delaying initiation of EE2 exposure from Day 4.0 gradually diminished the degree of feminization of ZZ-male gonads. Injection of vehicle emulsion without EE2 never affected morphological gonadal sex (data not shown). These observations indicate that ZZ-male gonads are sensitive to EE2-induced sex reversal only before completion of the morphological gonadal sex differentiation occurring on Days 6.0–7.0, which is indicated by the blue shade in Figure 1B [2].

ZZ-Male Embryonic Gonads Feminized by Exposure to EE2 Strongly Express Marker Genes for Ovarian Differentiation

Microarray profiling of normal gonadal transcriptomes on Day 19 showed extremely strong expression of the mRNA

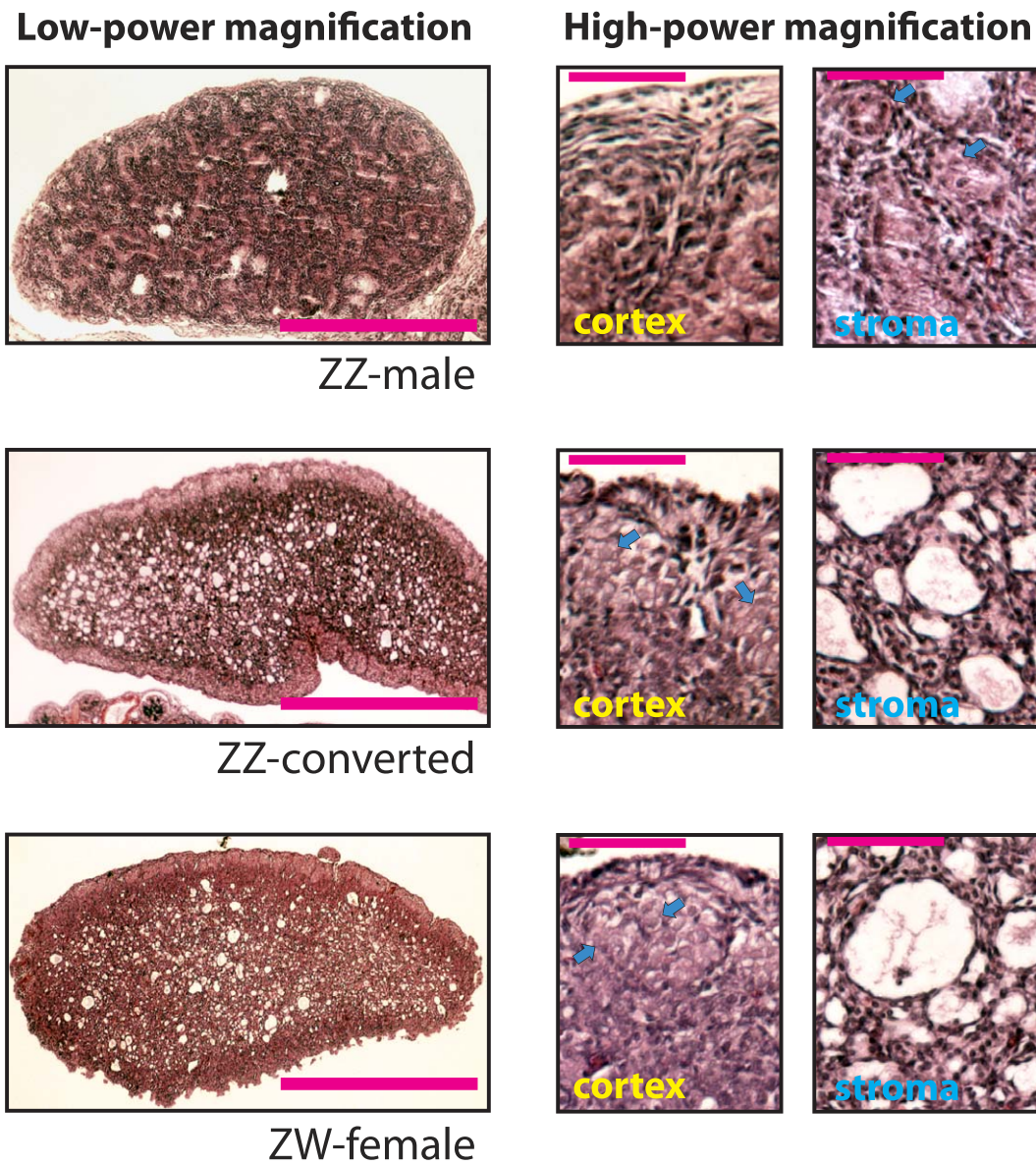


FIG. 2. Histological characteristics of chicken embryonic gonads at Day 19 of incubation using H&E staining. Bar indicates 0.5 mm (low-power panels) and 50 μ m (high-power panels), respectively. Blue arrows in the high-power panels indicate germline cells.

transcripts for *CYP19A1*/AROM and *FOXL2* in ovaries compared to testes (Fig. 3A). Expression of the mRNA transcripts for *SOX9*, a key transcription factor required for testicular sex differentiation [2], was stronger in ZZ testes than in ZW ovaries. Expression of several other mRNA transcripts involved in gonadal sex differentiation (reviewed in [1, 2]) differed by no greater than 2-fold between ZZ testes and ZW ovaries on Day 19.

The EE2-induced, complete morphological feminization of ZZ-male gonads was associated with strong expression of the mRNA transcripts for both *CYP19A1*/AROM and *FOXL2* to the levels indistinguishable from those in vehicle-injected ZW-female ovaries (Fig. 3B). Expression of these ovarian marker genes was completely suppressed to the levels in vehicle-injected ZZ-male testes when EE2 injection failed to induce morphological feminization because of delayed initiation of exposure. Expression of *ESR1* (encoding estrogen receptor α) in ZZ gonads was also enhanced to the normal ovarian level by the EE2-induced feminization although its sex-dependent difference was not as robust as *CYP19A1*/AROM or *FOXL2*.

Expression of *CYP17A1* (encoding 17 α -hydroxylase, a P450 enzyme required for androgen synthesis) was not affected by feminization.

EE2-Induced Feminization of ZZ-Male Embryonic Gonads Reduces Methylation at Specific CpG Dinucleotides in the CYP19A1 Promoter

To examine whether EE2-induced expression of *CYP19A1*/AROM mRNA in the feminized ZZ-male gonads is associated with changes in epigenetic marks on its promoter, methylation of CpG dinucleotides in *CYP19A1* promoter was determined by bisulfite pyrosequencing. The promoter of *ESR1*, whose expression was only modestly stronger in ZW ovaries compared to ZZ testes, was also included in the analysis. Figure 4A indicates positions of CpG dinucleotides in the *CYP19A1* and *ESR1* promoters around their transcription initiation sites (TISs). To our surprise, a 1-kbp region around the TIS of *CYP19A1* contained no CpG dinucleotide (shown by

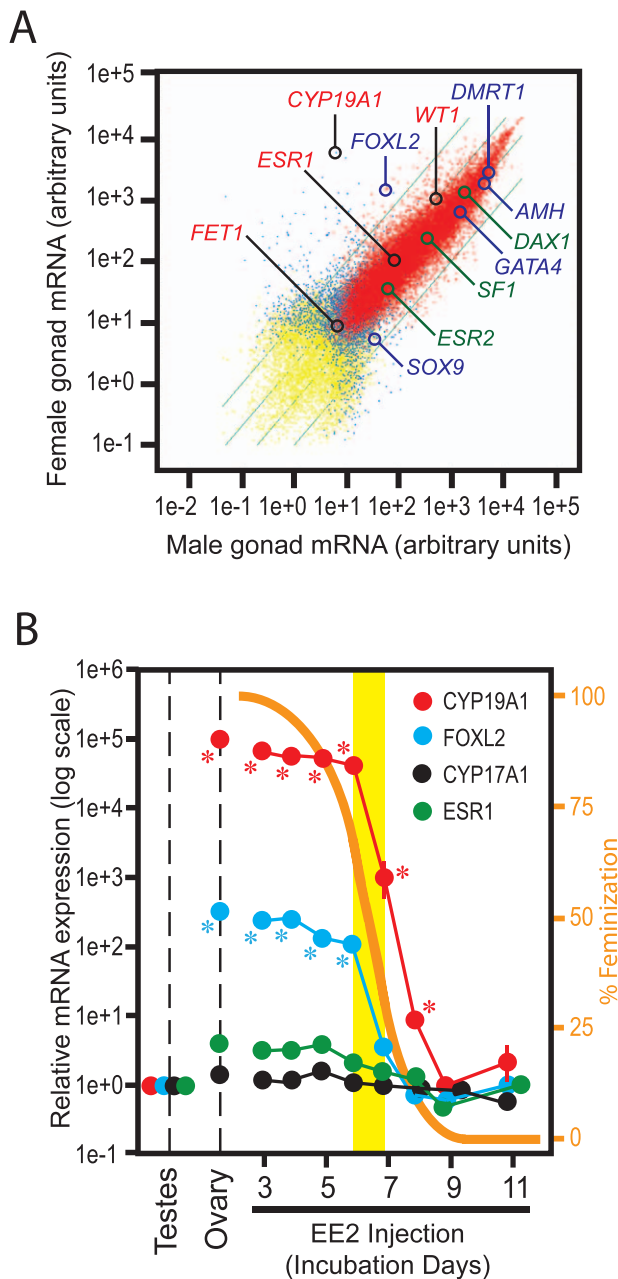


FIG. 3. Messenger RNA expression profiling of chicken embryonic gonads. **A**) Scatter plot of normal Day 19 ZZ-male and ZW-female gonadal transcriptomes determined by Affymetrix microarray. Red, blue, and yellow dots indicate mRNA expressed in both sexes, only one sex, or neither sex, respectively. Green lines indicate 2- and 10-fold differences between sexes. Datum points for key genes involved in chicken gonadal sex differentiation are indicated by circles. **B**) Expression of mRNA transcripts for *CYP19A1*/AROM, *FOXL2*, *CYP17A1*/17 α -hydroxylase, and *ESR1*/estrogen receptor α in Day 19 gonads of ZZ males exposed to EE2 (20 μ g/egg) from the indicated days of incubation. Orange curve and the right y-axis indicate degrees of morphological feminization shown in Figure 1B. Yellow band indicates the timing of gross morphological differentiation of normal testes (Day 6.0–7.0). Each datum point indicates mRNA expression relative to expression in testes of vehicle-exposed ZZ-male embryos (mean \pm SEM of five or more independent gonads). Messenger RNA expression in vehicle-exposed ZW-female ovaries is also shown. * $P < 0.05$ compared to vehicle-exposed ZZ-male testes (t -test).

horizontal bar). For this reason, 10 CpG sites most proximal upstream to the TIS were subjected to methylation analysis (boxed). For *ESR1*, methylation of 16 CpG sites in a DNA segment that included the TIS (boxed) was determined.

Among the 10 CpG sites in the *CYP19A1* promoter, the most distal five sites located 1400–1900 nt upstream to the TIS were strongly methylated (>60% methylation), showing no significant differences between ZZ testes, ZW ovaries, and completely sex-reversed ZZ gonads (Fig. 4B). In contrast, the CpG site 869 nt upstream to the TIS, CpG(–869), showed strongly sex-dependent differential methylation, namely, greater than 45% methylation in ZZ testes, 30%–35% methylation in completely sex-reversed ZZ gonads (feminization score = 3/3, or 100%), and less than 20% in ZW ovaries. The remaining four CpG sites were moderately methylated (>40%) with smaller degrees of sex-dependent differences. Bisulfite pyrosequencing of the same gDNA samples for CpG dinucleotides around the *ESR1* TIS revealed their strong hypomethylation without significant sex-dependent differences (Fig. 4C), demonstrating the specific nature of the sex-dependent hypomethylation of CpG (–869) in the *CYP19A1* promoter.

The sex-dependent differential methylation at and around CpG (–869) of the *CYP19A1* promoter in chicken embryonic gonads was further confirmed by independently performed experiments involving larger numbers of embryos (Fig. 4D). Thus, CpG (–869) was hypermethylated in vehicle-injected ZZ testes (51.3% \pm 0.8%; mean \pm SEM, $n = 20$), hypomethylated in vehicle-injected ZW ovaries (21.3% \pm 0.8%; $n = 24$), and methylated to an intermediate extent in completely sex-reversed ZZ-male gonads (34.0% \pm 2.4%; $n = 18$). Importantly, whereas these sex-reversed gonads were indistinguishable from vehicle-injected ZW ovaries by morphological and transcriptional criteria (see Figs. 1–3), the DNA methylation marks of CpG dinucleotides 955, 869, and 789 nt upstream of the TIS of the *CYP19A1* promoter never reached the degrees of hypomethylation observed with vehicle-injected ZW ovaries. In contrast, degrees of CpG (–869) methylation in heart muscle (left ventricle) were exactly the same between ZZ males and ZW females, showing slight hypomethylation compared to vehicle-injected ZZ testes (43%–45%) (Fig. 4D). The absence of the phenotypic sex-dependent differential methylation of CpG (–869) in the *CYP19A1* promoter was also observed in the liver (data not shown). Thus, DNA methylation at CpG (–955), CpG (–869), and CpG (–789) of the *CYP19A1* promoter reflected phenotypic gonadal sex differentiation in Day 19 chicken embryo whereas the same epigenetic marks showed no sex-dependent difference in other tissues than gonads.

To further characterize the EE2-induced *CYP19A1* promoter hypomethylation, we determined methylation at CpG (–869) and the two adjacent CpG sites of *CYP19A1* promoter in partially feminized ZZ gonads on Day 19 (Fig. 5). Methylation at these CpG sites was indistinguishable from that of vehicle-injected ZZ testes when EE2 exposure was delayed, initiating on Day 7 or later. Earlier initiation of exposure to EE2 caused hypomethylation of all three CpG sites although CpG (–869) was far more robustly hypomethylated than the other two CpG sites. Reproducing the results shown in Figure 4, B and D, hypomethylation of these three CpG sites was significant in the sex-reversed ZZ gonads but did not reach the very low levels of DNA methylation observed in the vehicle-injected ZW ovaries. Taken together, these results confirmed that the *CYP19A1* promoter is hypomethylated at specific CpG sites when ZZ gonads are sex-reversed by exposure to EE2 prior to completion of morphological sex differentiation whereas the maximum degrees of such EE2-induced hypomethylation do not reach to the levels of DNA hypomethylation observed in genetically female ZW ovaries.

To obtain further insights into the mechanism of the sex-specific differential DNA methylation observed in the

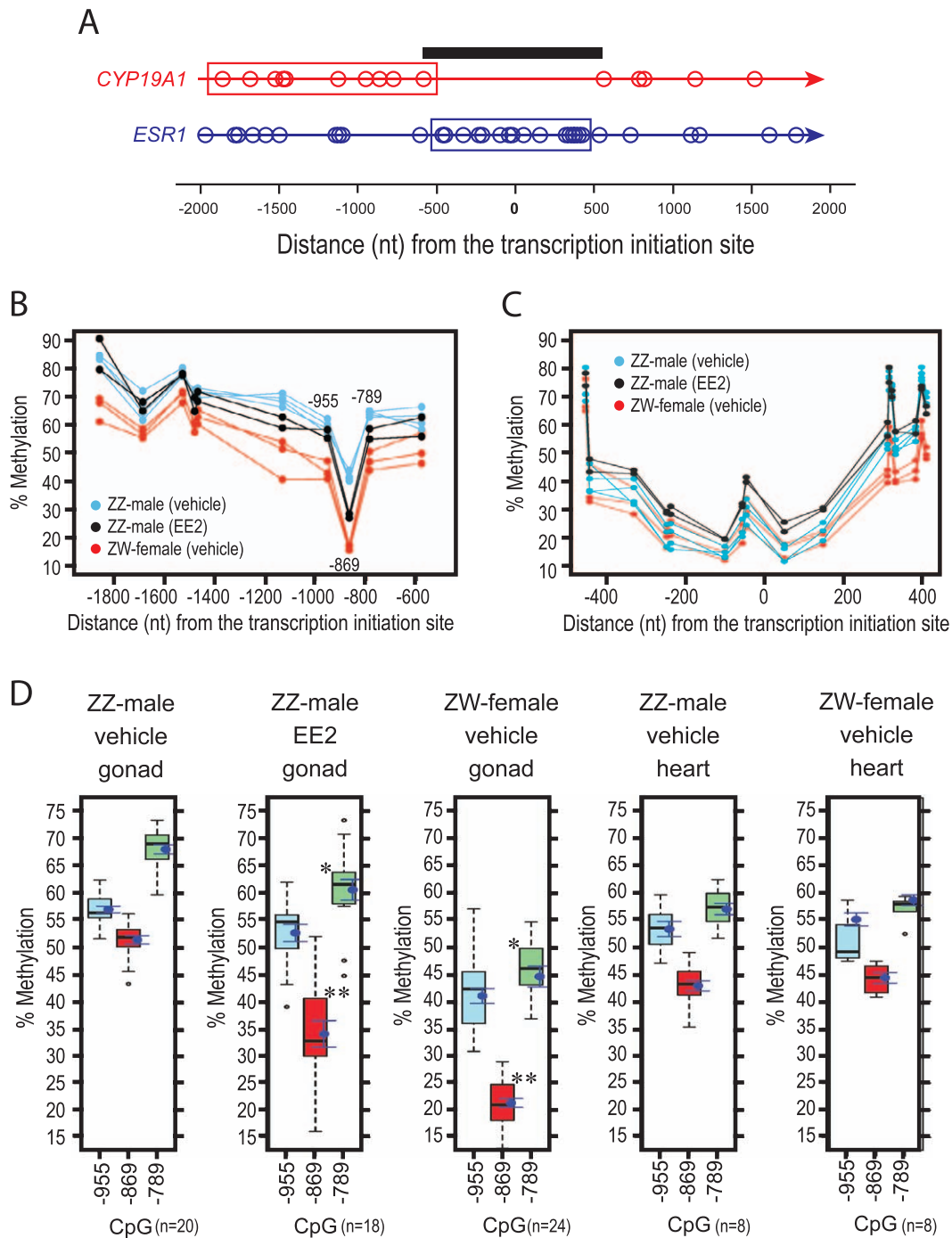


FIG. 4. DNA methylation profiling of chicken embryonic gonads. **A**) Positions of CpG dinucleotides in the *CYP19A1* and *ESR1* promoters around the TISs. Boxes indicate DNA segments subjected to bisulfite pyrosequencing shown in **B–D**. Horizontal bar indicates a 1-kb CpG-free region in the *CYP19A1* promoter. **B, C**) CpG methylation in the promoters of *CYP19A1* (**B**) and *ESR1* (**C**) in Day 19 gonads of chicken embryos exposed to EE2 (20 μ g/egg) or vehicle from Day 3. Percent methylation values of each datum point were determined by triplicate pyrosequencing assays. Numbers in **B** indicate nucleotide base positions of the CpG sites relative to the TIS. **D**) DNA methylation of CpG dinucleotides located 955, 869, and 789 nt upstream of the TIS of the *CYP19A1* promoter in gonads or left ventricular heart muscle of Day 19 embryos exposed to EE2 (20 μ g/egg) or vehicle from Day 3. Box plot indicates median, quarterly boundaries, and ranges. Dot and bar indicates mean \pm SEM; numbers of individual embryos involved in each plot are indicated in parentheses. * $P < 0.05$ and ** $P < 0.01$ compared to gonads of vehicle-exposed ZZ-male embryos (t-test).

CYP19A1 promoter, we examined mRNA expression and DNA methylation status of the *DNMT* family of genes encoding the DNA methyltransferases. Expression of the mRNA transcripts for the DNMT1 maintenance DNA methyltransferase and the DNMT3A and DNMT3B de novo DNA methyltransferases were not significantly affected by either the genetic sex or EE2-induced sex conversion (Supplementary Figure S1). Therefore,

the sex-dependent differential methylation in the *CYP19A1* promoter was not explained by changes in the *DNMT* mRNA expression. We next determined DNA methylation status in the first exon of the de novo DNA methyltransferase genes using the pyrosequencing assay described by Yu et al. [32]. As shown in Supplementary Figure S2, neither *DNMT3A* nor *DNMT3B* genes showed significant sex-dependent differences

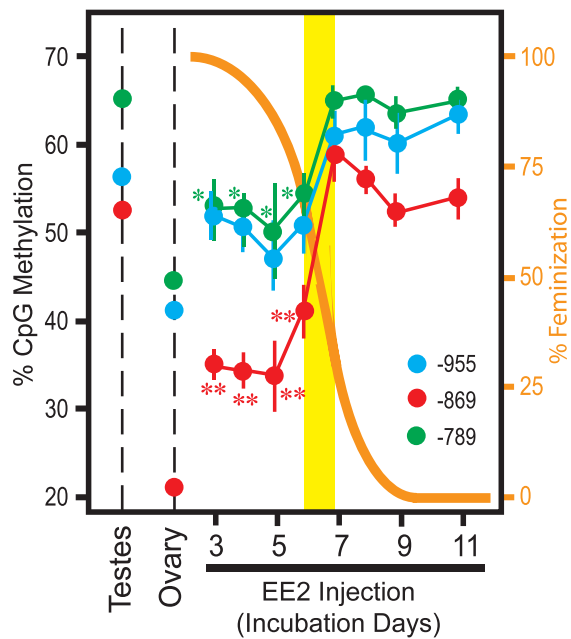


FIG. 5. DNA methylation at CpG (-955), CpG (-869), and CpG (-789) of the *CYP19A1* promoter in Day 19 gonads of ZZ-male chicken embryos exposed to EE2 (20 $\mu\text{g}/\text{egg}$) from the indicated days of incubation. Orange curve and the right y-axis indicate degrees of morphological feminization shown in Figure 1B. Each datum point indicates DNA methylation at CpG sites 955, 869, or 789 nt upstream of the *CYP19A1* TIS (mean \pm SEM of five or more independent gonads). CpG methylation in vehicle-exposed ZZ-male testes and ZW-female ovaries are also shown. * $P < 0.05$ and ** $P < 0.01$ compared to vehicle-exposed ZZ-male testes (*t*-test).

in their first exon methylation. Note that the *DNMT3B* data presented here do not contain polymorphic CpG dinucleotides whose cytosine is often substituted with adenine or guanine as previously described [32] and confirmed by our experiments (data not shown). The absence of sex-dependent differential DNA methylation in these genes further supports the highly specific nature of the sex-dependent epigenetic markers in the *CYP19A1* promoter.

EE2-Induced Partial Hypomethylation of the *CYP19A1* Promoter Is Observed in Germline-Depleted Gonadal Somatic Cells

The chicken gonadal tissue consists of two distinct types of cells, namely, germline cells and somatic cells. When chicken primordial germ cells (PGCs) are conveyed from the epiblast into the genital ridge through the bloodstream, both ZZ PGCs and ZW PGCs are still sexually bipotential and capable of differentiating into both male and female germline lineages [2]. When gonadal somatic cells undergo sex differentiation, the phenotypic sex of the PGCs is determined by the sex of the somatic cells surrounding them [2]. Therefore, EE2-induced feminization of ZZ-male gonads is presumed to occur primarily in the gonadal somatic cells. We considered the possibility that the incomplete epigenetic sex conversion of the *CYP19A1* promoter observed with the whole-gonadal tissue samples (Figs. 4 and 5) might be explained if gonadal somatic cells could actually undergo complete epigenetic sex conversion whereas germline cells do not. To address this possibility, SSEA-1 positive germline cells were depleted from single cell suspensions of Day 19 chicken embryonic gonads by a MACS system using a monoclonal antibody to SSEA-1, a glycoprotein marker antigen specifically expressed in germline cells in

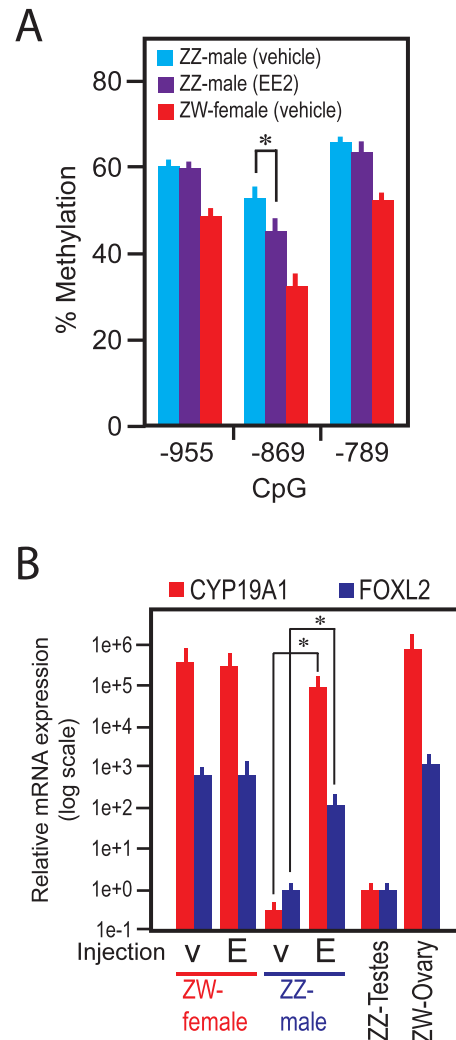


FIG. 6. DNA methylation and mRNA expression in Day 19 germline-depleted gonadal cells in chicken embryos. **A**) DNA methylation at CpG sites 955, 869, or 789 nucleotides upstream of the *CYP19A1* TIS in germline-depleted gonadal somatic cells. Embryos were exposed to EE2 (20 $\mu\text{g}/\text{egg}$) or vehicle from Day 3. Data indicate CpG methylation on Day 19 (mean \pm SEM of five or more independent gonads). * $P < 0.05$ (*t*-test). **B**) Expression of mRNA transcripts for *CYP19A1*/aromatase and *FOXL2* in germline-depleted gonadal somatic cells of chicken embryos exposed to EE2 (20 $\mu\text{g}/\text{egg}$) or vehicle from Day 3. Messenger RNA expression in total testes and ovaries of control animals is also shown. Data indicate relative mRNA expression compared to that in Day 19 total testes of vehicle-exposed ZZ males and are presented in log scale (mean \pm SEM of five or more independent gonads).

mammalian and chicken embryonic gonads [34] (Supplementary Fig. S3A). Two consecutive MACS runs yielded germline-free gonadal somatic cells showing less than 0.1% of contamination of SSEA-1 positive, fluorescent cells (Supplementary Fig. S3B). Germline-enriched cells showed contamination of up to 30% fluorescence-negative cells.

DNA methylation profiles of the *ESR1* promoter were clearly different between the germline-enriched cells and the germline-depleted somatic cells (Supplementary Fig. S3C). The strong CpG methylation immediately before the TIS in the germline-enriched cells may reflect the absence of germline expression of estrogen receptor α [2]. The similarity in the *ESR1* promoter methylation in the germline-depleted somatic cells and the whole gonads (Supplementary Fig. S3C, center panel; compare with Fig. 4C) suggests the dominance of

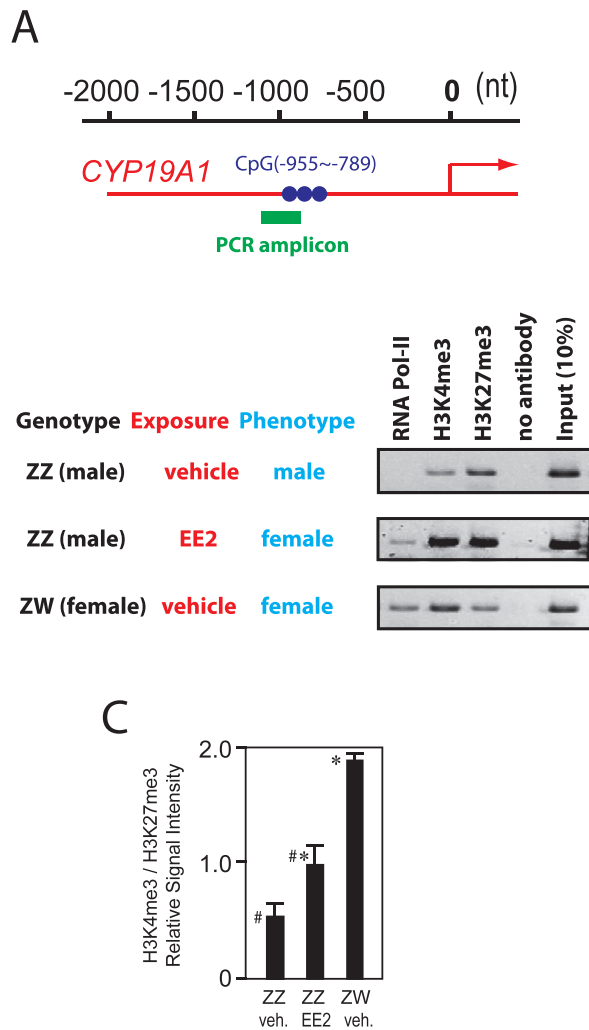


FIG. 7. Pro- and antitranscriptional histone modifications and RNA polymerase II recruitment to the *CYP19A1* promoter in Day 19 chicken embryonic gonads. **A**) Position of the PCR amplicon for the ChIP assay. Circles indicate the three CpG sites 955, 869, or 789 nt upstream of the TIS of the *CYP19A1* promoter (indicated by arrow). **B**) ChIP assay for trimethylated H3K4 (protranscriptional), H3K27 (antitranscriptional), and RNA polymerase II recruitment to the *CYP19A1* promoter in Day 19 chicken gonads of ZZ males, ZW females, and EE2-exposed, completely sex-converted ZZ males. Inverted images of agarose gel electrophoresis of the PCR products are shown. **C**) Relative signals for H3K4me3 and H3K27me3 of **B** determined by densitometry (mean \pm SEM of ChIP assays on three independent gonads for each group). # and * indicate statistically significant differences ($P < 0.05$, t -test).

somatic cells compared to germline cells in Day 19 gonads. In contrast, the *CYP19A1* promoter methylation profiles determined using the same genomic DNA samples were similar between the germline-enriched cells and the germline-depleted somatic cells (Supplementary Figure S3D). Detailed methylation analyses on CpG (-869) and the adjacent two CpG sites in the *CYP19A1* promoter demonstrated significant but moderate hypomethylation of CpG (-869) in the germline-depleted somatic cells isolated from completely feminized ZZ-male gonads exposed to EE2 from Day 3 (Fig. 6A), reproducing the observations made with the whole gonadal tissues (see Figs. 4 and 5). These results indicate that the difference in the degree of the *CYP19A1* promoter hypomethylation between the completely feminized ZZ gonads by exposure to EE2 and the gonads of vehicle-injected ZW-female embryos directly reflected the epigenetic status in the gonadal somatic cells

with negligible bias derived from the germline cells. The EE2-induced expression of the mRNA transcripts for *CYP19A1*/AROM and FOXL2 observed with the whole-gonadal tissue specimens (Figs. 4 and 5) was reproduced with the germline-depleted somatic cells (Fig. 6B), indicating that both the EE2-induced hypomethylation of the *CYP19A1* promoter and the concomitant, robust expression of these two marker genes of ovarian differentiation were derived from changes in the gonadal somatic cells. Because of the significant contamination of the gonadal somatic cells in the SSEA-1 positive germline-enriched cell preparations, their transcriptional and DNA methylation analyses were inconclusive (data not shown).

EE2-Induced Feminization of ZZ-Male Embryonic Gonads Involves Protranscriptional Histone Modifications in the *CYP19A1* Promoter

To obtain insights into whether the EE2-induced DNA hypomethylation in the *CYP19A1* promoter in ZZ-male gonads is mechanistically linked to the concomitant and strong expression of the *CYP19A1*/AROM mRNA transcripts, histone modifications (protranscriptional H3K4me3 and antitranscriptional H3K27me3) and RNA polymerase II recruitment to *CYP19A1* promoter in Day 19 chicken embryonic gonads were examined by ChIP assay. To our surprise, extensive analyses around the ovary-specific TIS of the *CYP19A1* promoter as reported by Matsumine et al. [35] detected neither sexual dimorphism in the H3K4me3/H3K27me3 ratio nor RNA polymerase II recruitment (data not shown). Interestingly, however, ChIP assays targeting a promoter sequence involving the three sex-dependent, differentially methylated CpG sites (Fig. 7A) did show sex-dependent changes in the H3K4me3/H3K27me3 ratio and phenotypic feminization-dependent recruitment of RNA polymerase II (Fig. 7, B and C). In ZZ-male gonads, H3 histones in this region were predominantly methylated at the antitranscriptional lysine-27, and no RNA polymerase II recruitment was detected. In contrast, in ZW-female gonads, H3 histones in the same region were predominantly methylated at the protranscriptional lysine-4, and recruitment of RNA polymerase II was readily detected. In the EE2-exposed, feminized ZZ gonads, histone H3 was methylated at both lysine-4 and lysine-27 with comparable strength, and significant recruitment of RNA polymerase II was also detected. Thus, not only DNA methylation but also histone H3 modifications at this specific region in the *CYP19A1* promoter demonstrated significant but incompletely feminized profiles. These results suggest that the sexually dimorphic epigenetic marks of this region in the *CYP19A1* promoter may play mechanistic roles in the strong expression of the *CYP19A1*/AROM mRNA transcripts characteristic to the phenotypically female chicken embryonic gonads.

DISCUSSION

In chicken embryonic gonads, sexual dimorphism at the level of marker gene expression occurs long before the morphological sexual differentiation initiates on Day 6.0–6.5. The masculinizing gene *DMRT1* and the ovarian marker genes *ASW* and *FET1* already show genetic sex-dependent differential mRNA expression in gonads on Day 3.5 when ZZ gonads and ZW gonads are still morphologically indistinguishable [1, 2]. In the present study, we observed morphologically and transcriptionally complete male-to-female gonadal sex reversal in chicken embryos exposed to EE2 no later than Day 4.0 (Figs. 1 and 3). When EE2 exposure is initiated immediately before the gonadal morphological sex differentiation on Day

6.0, morphological feminization was slightly suppressed when it was evaluated using our arbitrary scoring system (Fig. 1) whereas mRNA expression of the key ovarian genes *CYP19A1*/AROM and *FOXL2* was completely feminized (Fig. 3). A dramatic gain of resistance to the EE2-induced feminization of ZZ gonads occurred within a narrow window between Days 6.0 and 7.0 in both morphological and mRNA expression criteria. This timing matches initiation of normal expression of *SOX9*, a SOX family transcription factor well conserved among reptiles, birds, and mammals, and expressed exclusively in the Sertoli cell lineage of the medullary cords of male gonads [36]. The Sertoli cell is the first cell type to differentiate in male gonads that sets a cascade of cellular events resulting in testes differentiation [37]. Thus, EE2-induced morphological and transcriptional feminization of ZZ gonads is capable of overcoming effects of the early expression of the masculinizing genes *DMRT1* (Day ~3.5) and anti-Müllerian hormone (*AMH*, Day ~5.0) [2], but cannot reverse the masculinizing cascade once *SOX9* initiates Sertoli cell differentiation.

Whereas exposure of ZZ gonads to EE2 from as early as Day 3.0 resulted in complete morphological and transcriptional feminization observed with Day 19 gonads, the epigenetic sex marks in the promoter of the *CYP19A1* gonadal feminizing gene was clearly incomplete, showing an intermediate level of DNA methylation and histone lysine methylation between the normal ZZ gonads and the normal ZW gonads (Figs. 4 and 5). Taken together, these observations suggest that, even when the exogenous EE2 triggered a feminizing cascade of molecular events through a shortcut activation of estrogen receptor α in the gonadal cortex [2] and suppressed progression of the genetically dictated masculinizing cascade as long as *SOX9* expression was not initiated yet, the early events of gonadal masculinization initiated by *DMRT1* may still affect the epigenetic mechanisms regulating expression of *CYP19A1*/AROM, leaving the persistent, intermediate epigenetic sex marks in its promoter. Previous studies observed that estrogen-induced gonadal feminization of ZZ-male chicken embryos often diminishes after hatching and during puberty of the birds [3]. The incomplete aspect of the epigenetic sex reversal in the *CYP19A1* promoter (and probably other persistent, promasculinizing epigenetic marks regulating expression of other key sex-determining genes as well) may explain the unstable nature of the estrogen-induced feminization of ZZ gonads.

Our pyrosequencing analyses on EE2-induced hypomethylation in the *CYP19A1* promoter with nucleotide-base resolution power revealed that significant phenotypic sex-dependent differences in DNA methylation were restricted to less than six CpG dinucleotides within a 1.2-kb sequence (Fig. 4B). The most informative three CpG sites, -955, -869, and -789 nt upstream of the TIS (Figs. 4, B and D, and 5), were located within only a 170-nt segment flanked with hypermethylated segments. Furthermore, the phenotypic sex-dependent differences in methylation of these CpG sites were not dichotomous (i.e., zero methylation versus total methylation) but only quantitative although they were significant and highly reproducible (Fig. 4D). These features of the epigenetic sex marks identified in the present study may explain our multiple but unsuccessful attempts to detect phenotypic sex-dependent differences in DNA methylation by the microarray analysis of methylated DNA immunoprecipitation approach (data not shown), whose power to distinguish methylation status of a specific CpG dinucleotide is strongly affected by methylation of the surrounding DNA segments [38]. Our results were similar to those reported by Dolinoy et al. [39, 40], who determined changes in methylation of only nine CpG dinucleotides in the *agouti* pseudoexon 1A promoter of *A^{vy/a}*

mice induced by fetal exposure to estrogenic endocrine disruptors, demonstrating distinct sensitivities of the individual CpG sites for estrogen-induced methylation. Epigenetic effects of embryonic exposure to environmental agents in the vertebrate genomes might be sometimes restricted to small numbers of specific CpG sites rather than affecting relatively large numbers of CpG sites within long genomic DNA segments. Recent progress in research on the environmental endocrine disruptors, including EE2 as one of the strongest estrogenic environmental pollutants, has developed a paradigm that embryonic or fetal exposure of vertebrates to certain types of environmental endocrine disruptors may cause persistent changes in the epigenetic mechanisms regulating gene expression in the embryonic/fetal genome [39, 41–43]. Interestingly, an increasing number of studies propose that epigenetic changes introduced into the genome of germline cells by environmental epimutagens might be transgenerationally transmitted and cause disorders in the unexposed generations of the offspring [44–47]. Debates are ongoing as to whether such transgenerationally transmitted, disease-relevant epimutations may require specific genetic backgrounds of the laboratory animals [48] or might not occur as significant threats to human and wildlife health with environmentally relevant concentrations of the epimutagens chemicals [49]. Our present study demonstrates the importance of examining changes in DNA methylation and other epigenetic marks caused by fetal exposure to environmental factors with the single nucleotide resolution power using the latest high-throughput technologies, including base-specific cleavage mass spectrometry [47, 50] and bisulfite deep sequencing [51–53] in addition to the standard bisulfite pyrosequencing approach. Future studies should address the mechanistic basis of this apparent nucleotide-level specificity of epigenetic effects of embryonic exposure to environmental hormonal agents. Establishing comprehensive methods of nucleotide-resolution epigenetic analysis would also be important to determine whether multigenerational effects observed after exposure of vertebrate embryos/fetuses to environmental factors are epigenetically transmitted [44–47] or occur through alternative mechanisms as recently reported [54, 55].

Chicken embryonic gonads at Day 19 consist of multiple types of heterogeneous cells. Although our present study demonstrated that the aspects of epigenetic sex determined with the whole gonadal tissue samples were not significantly affected by depletion of the SSEA1-positive germline cells from the analysis (Fig. 6), the somatic cell population itself is still heterogeneous, consisting of cells in the cortex, the medullary cords, and the medullary stroma. Because histological observations did not find any significant differences between the EE2-feminized ZZ gonads and the control ZW gonads (Fig. 2), we presume that the quantitative differences in the epigenetic sex marks of the *CYP19A1* promoter between these gonads were not primarily due to different ratios of the heterogeneous cell types. However, it remains to be determined by future studies as to whether such heterogeneous subpopulations of the gonadal somatic cells share a single pattern of common epigenetic sex marks or not.

The discrepancy between the curves for AROM mRNA expression (Fig. 3B) and DNA methylation of the epigenetic sex marks in its promoter (Fig. 5) plotted using the same abscissa (initiation of EE2 exposure) may suggest that moderate hypomethylation of this promoter may be sufficient to release it from epigenetic transcriptional suppression. On the other hand, it is tempting to speculate that the EE2-feminized ZZ gonads might be more sensitive to endogenous and exogenous factors that repress transcription of the *CYP19A1*/

AROM gene than normal ZW gonads because of the significantly more methylated status of this promoter. In this context, it is interesting that we were unable to detect RNA polymerase II recruitment to the previously reported TIS of the *CYP19A1* promoter whereas we did detect it about 1-kb upstream to the TIS (Fig. 7 and data not shown). The ovarian TIS of chicken *CYP19A1* promoter (nucleotide position 6,293,986 of NCBI Reference Sequence NW_003763854.1, *Gallus gallus* 4.0 whole genome shotgun sequence) was determined by Matsumine et al. [35] using a primer extension method, which was not designed to detect possibly another TIS 1-kb upstream of their RNA hybridization primer. Unfortunately, because the longest mRNA transcript for chicken *CYP19A1*/AROM registered in the publicly available databases starts at nucleotide position 6,293,942 of the same contig, which is even 44 nucleotides shorter than the transcript reported by Matsumine et al. [35], whether a true TIS of this gene locates near the CpG sites about 1-kb upstream of the previously reported TIS is left undetermined. Our multiple attempts to determine such a novel TIS by primer extension and other approaches have not been successful, possibly reflecting a short length of the first exon that is experimentally challenging to determine. The apparent discrepancy between our present study and the report of Matsumine et al. [35] might reflect possible differences in the transcriptional activity of the *CYP19A1* gene in the embryonic chicken gonads and the ovaries of matured female chickens.

At present, a mechanistic explanation about how exposure to EE2 results in highly specific changes in the epigenetic status of the *CYP19A1* promoter is unavailable although previous studies suggests roles of estrogen receptor α in the mechanism of male-to-female sex reversal by exogenous estrogens [2]. Estrogen-dependent DNA demethylation in vertebrate cells has been known for over three decades. Estrogen-dependent demethylation of chicken vitellogenin promoter in the egg-laying hen is known to occur after its transcriptional activation by ligand-activated estrogen receptor without requiring DNA synthesis [56–58]. In human cells, the estrogen-responsive promoter of the pS2 gene undergoes rapid and cyclic changes in DNA methylation that are synchronized with cyclic recruitment of ligand-activated estrogen receptor α and RNA polymerase II [59, 60]. In the estrogen-dependent human MCF-7 breast cancer cells, activation of the cathepsin D gene is associated with rapid demethylation of its distal enhancer, which contains the estrogen responsive element and is known as a direct target of the estrogen receptors [61]. These studies suggest that estrogen might control DNA methylation through estrogen receptor-mediated events of transcriptional activation, which involves formation of a number of multi-protein complexes that could contain subunits that affect cytosine methylation of the targeted chromatin segments. The phenotypic sex-dependent DNA methylation marks in the *CYP19A1* promoter described in the present study could also be explained in the context of estrogen-induced demethylation of the regulatory elements of transcriptionally active genes.

Recently, proposed possible roles of the TET-family methylcytosine hydroxylases and the hydroxymethylcytosines in active and sequence-specific DNA demethylation [62] might also be relevant to the EE2-induced epigenetic changes, which should be addressed by future studies. Bannister et al. [63] recently reported that chicken micro-RNA MIR202*, which shows sexually dimorphic expression in embryonic chicken gonads (testis-specific) and reduces its expression upon estradiol-induced feminization of ZZ gonads [64], enhances expression of testis-associated genes DMRT1 and SOX9 and suppresses ovary-associated genes FOXL2 and *CYP19A1*/

AROM [64]. It would be important to establish how different types of epigenetic mechanisms—namely, DNA methylation/hydroxymethylation, histone modifications, and micro-RNA—regulate expression of key sex determination genes in coordinating manners.

In summary, our present study demonstrated that changes in DNA methylation associating phenotypic sex differentiation of chicken embryonic gonads can occur within a very short length of chromatin segment that may contain only a few CpG dinucleotides. Such changes in DNA methylation occur in a highly quantitative manner and are appropriately evaluated with the bisulfite-pyrosequencing technology. The morphological, transcriptomal, genetic, and epigenetic sex may not agree with each other when gonadal sex differentiation is disturbed by exogenous factors; the phenotypic sex (i.e., morphological and transcriptomal sex marks) can be completely reversed whereas epigenetic sex marks tend to be persistent with the original, genetically dictated sex. These findings provide critical insights into roles of the epigenetic mechanisms of normal gonadal development and their disruption by exogenous factors, emphasizing the importance of evaluating epigenetic events in a highly quantitative manner with nucleotide base-level resolution for the assessment of environmental toxicants as developmental epimutagens.

ACKNOWLEDGMENT

We thank Crystal Mahoney, Sabrina Collins, and Shannon Smith for their technical assistance.

REFERENCES

- Smith CA, Roeszler KN, Hudson QJ, Sinclair AH. Avian sex determination: what, when and where? *Cytogenet Genome Res* 2007; 117:165–173.
- Smith CA, Sinclair AH. Sex determination: insights from the chicken. *Bioessays* 2004; 26:120–132.
- Scheib D. Effects and role of estrogens in avian gonadal differentiation. *Differentiation* 1983; 23(Suppl):S87–S92.
- Teng CS, Teng CT. Decreased ovalbumin-gene response to oestrogen in the prenatally diethylstilboestrol-exposed chick oviduct. *Biochem J* 1985; 228:689–695.
- Berg C, Halldin K, Brunstrom B. Effects of bisphenol A and tetrabromobisphenol A on sex organ development in quail and chicken embryos. *Environ Toxicol Chem* 2001; 20:2836–2840.
- Berg C, Halldin K, Fridolfsson AK, Brandt I, Brunstrom B. The avian egg as a test system for endocrine disruptors: effects of diethylstilbestrol and ethynylestradiol on sex organ development. *Sci Total Environ* 1999; 233: 57–66.
- Smith CA, Katz M, Sinclair AH. DMRT1 is upregulated in the gonads during female-to-male sex reversal in ZW chicken embryos. *Biol Reprod* 2003; 68:560–570.
- Elbrecht A, Smith RG. Aromatase enzyme activity and sex determination in chickens. *Science* 1992; 255:467–470.
- Vaillant S, Magre S, Dorizzi M, Pieau C, Richard-Mercier N. Expression of AMH, SF1, and SOX9 in gonads of genetic female chickens during sex reversal induced by an aromatase inhibitor. *Dev Dyn* 2001; 222:228–237.
- Hudson QJ, Smith CA, Sinclair AH. Aromatase inhibition reduces expression of FOXL2 in the embryonic chicken ovary. *Dev Dyn* 2005; 233:1052–1055.
- Vaillant S, Dorizzi M, Pieau C, Richard-Mercier N. Sex reversal and aromatase in chicken. *J Exp Zool* 2001; 290:727–740.
- Nakabayashi O, Kikuchi H, Kikuchi T, Mizuno S. Differential expression of genes for aromatase and estrogen receptor during the gonadal development in chicken embryos. *J Mol Endocrinol* 1998; 20:193–202.
- Smith CA, Andrews JE, Sinclair AH. Gonadal sex differentiation in chicken embryos: expression of estrogen receptor and aromatase genes. *J Steroid Biochem Mol Biol* 1997; 60:295–302.
- Nishikimi H, Kansaku N, Saito N, Usami M, Ohno Y, Shimada K. Sex differentiation and mRNA expression of P450c17, P450arom and AMH in gonads of the chicken. *Mol Reprod Dev* 2000; 55:20–30.
- Andrews JE, Smith CA, Sinclair AH. Sites of estrogen receptor and

- aromatase expression in the chicken embryo. *Gen Comp Endocrinol* 1997; 108:182–190.
16. Govoroun MS, Pannetier M, Pailhoux E, Cocquet J, Brillard JP, Couty I, Batellier F, Cotinot C. Isolation of chicken homolog of the FOXL2 gene and comparison of its expression patterns with those of aromatase during ovarian development. *Dev Dyn* 2004; 231:859–870.
 17. Loffler KA, Zarkower D, Koopman P. Etiology of ovarian failure in blepharophimosis ptosis epicanthus inversus syndrome: FOXL2 is a conserved, early-acting gene in vertebrate ovarian development. *Endocrinology* 2003; 144:3237–3243.
 18. Smith CA, Roeszler KN, Ohnesorg T, Cummins DM, Farlie PG, Doran TJ, Sinclair AH. The avian Z-linked gene DMRT1 is required for male sex determination in the chicken. *Nature* 2009; 461:267–271.
 19. Yang X, Zheng J, Qu L, Chen S, Li J, Xu G, Yang N. Methylation status of cMHM and expression of sex-specific genes in adult sex-reversed female chickens. *Sex Dev* 2011; 5:147–154.
 20. Chue J, Smith CA. Sex determination and sexual differentiation in the avian model. *FEBS J* 2011; 278:1027–1034.
 21. Yang X, Zheng J, Xu G, Qu L, Chen S, Li J, Yang N. Exogenous cMHM regulates the expression of DMRT1 and ER alpha in avian testes. *Mol Biol Rep* 2010; 37:1841–1847.
 22. Rosenthal NF, Ellis H, Shioda K, Mahoney C, Coser KR, Shioda T. High-throughput applicable genomic sex typing of chicken by TaqMan real-time quantitative polymerase chain reaction. *Poult Sci* 2010; 89:1451–1456.
 23. Halldin K, Berg C, Brandt I, Brunstrom B. Sexual behavior in Japanese quail as a test end point for endocrine disruption: effects of in ovo exposure to ethinylestradiol and diethylstilbestrol. *Environ Health Perspect* 1999; 107:861–866.
 24. McKernan MA, Rattner BA, Hale RC, Ottinger MA. Egg incubation position affects toxicity of air cell administered polychlorinated biphenyl 126 (3,3',4,4',5-pentachlorobiphenyl) in chicken (*Gallus gallus*) embryos. *Environ Toxicol Chem* 2007; 26:2724–2727.
 25. Kim JN, Park TS, Park SH, Park KJ, Kim TM, Lee SK, Lim JM, Han JY. Migration and proliferation of intact and genetically modified primordial germ cells and the generation of a transgenic chicken. *Biol Reprod* 2009; 82:257–262.
 26. Kim H, Park TS, Lee WK, Moon S, Kim JN, Shin JH, Jung JG, Lee SD, Park SH, Park KJ, Kim MA, Shin SS, et al. MPSS profiling of embryonic gonad and primordial germ cells in chicken. *Physiol Genomics* 2007; 29: 253–259.
 27. Kim JN, Kim MA, Park TS, Kim DK, Park HJ, Ono T, Lim JM, Han JY. Enriched gonadal migration of donor-derived gonadal primordial germ cells by immunomagnetic cell sorting in birds. *Mol Reprod Dev* 2004; 68: 81–87.
 28. Pesce M, De Felici M. Purification of mouse primordial germ cells by MiniMACS magnetic separation system. *Dev Biol* 1995; 170:722–725.
 29. Coser KR, Chesnes J, Hur J, Ray S, Isselbacher KJ, Shioda T. Global analysis of ligand sensitivity of estrogen inducible and suppressible genes in MCF7/BUS breast cancer cells by DNA microarray. *Proc Natl Acad Sci U S A* 2003; 100:13994–13999.
 30. Coser KR, Wittner BS, Rosenthal NF, Collins SC, Melas A, Smith SL, Mahoney CJ, Shioda K, Isselbacher KJ, Ramaswamy S, Shioda T. Antiestrogen-resistant subclones of MCF-7 human breast cancer cells are derived from a common monoclonal drug-resistant progenitor. *Proc Natl Acad Sci U S A* 2009; 106:14536–14541.
 31. Shioda T, Chesnes J, Coser KR, Zou L, Hur J, Dean KL, Sonnenschein C, Soto AM, Isselbacher KJ. Importance of dosage standardization for interpreting transcriptomal signature profiles: evidence from studies of xenoestrogens. *Proc Natl Acad Sci U S A* 2006; 103:12033–12038.
 32. Yu Y, Zhang H, Tian F, Zhang W, Fang H, Song J. An integrated epigenetic and genetic analysis of DNA methyltransferase genes (DNMTs) in tumor resistant and susceptible chicken lines. *PLoS One* 2008; 3:e2672.
 33. Yahata T, Shao W, Endoh H, Hur J, Coser KR, Sun H, Ueda Y, Kato S, Isselbacher KJ, Brown M, Shioda T. Selective coactivation of estrogen-dependent transcription by CITED1 CBP/p300-binding protein. *Genes Dev* 2001; 15:2598–2612.
 34. Jung JG, Kim DK, Park TS, Lee SD, Lim JM, Han JY. Development of novel markers for the characterization of chicken primordial germ cells. *Stem Cells* 2005; 23:689–698.
 35. Matsumine H, Herbst MA, Ou SH, Wilson JD, McPhaul MJ. Aromatase mRNA in the extragonadal tissues of chickens with the henly-feathering trait is derived from a distinctive promoter structure that contains a segment of a retroviral long terminal repeat. Functional organization of the Sebright, Leghorn, and Campine aromatase genes. *J Biol Chem* 1991; 266: 19900–19907.
 36. Kent J, Wheatley SC, Andrews JE, Sinclair AH, Koopman P. A male-specific role for SOX9 in vertebrate sex determination. *Development* 1996; 122:2813–2822.
 37. Skinner MK, Griswold MD (eds.). *Sertoli Cell Biology*. San Diego: Elsevier Academic Press; 2005.
 38. Pelizzola M, Koga Y, Urban AE, Krauthammer M, Weissman S, Halaban R, Molinaro AM. MEDME: an experimental and analytical methodology for the estimation of DNA methylation levels based on microarray derived MeDIP-enrichment. *Genome Res* 2008; 18:1652–1659.
 39. Dolinoy DC, Huang D, Jirtle RL. Maternal nutrient supplementation counteracts bisphenol A-induced DNA hypomethylation in early development. *Proc Natl Acad Sci U S A* 2007; 104:13056–13061.
 40. Dolinoy DC, Weidman JR, Waterland RA, Jirtle RL. Maternal genistein alters coat color and protects Avy mouse offspring from obesity by modifying the fetal epigenome. *Environ Health Perspect* 2006; 114: 567–572.
 41. Dolinoy DC, Weidman JR, Jirtle RL. Epigenetic gene regulation: linking early developmental environment to adult disease. *Reprod Toxicol* 2007; 23:297–307.
 42. Diamanti-Kandaraki E, Bourguignon JP, Giudice LC, Hauser R, Prins GS, Soto AM, Zoeller RT, Gore AC. Endocrine-disrupting chemicals: an Endocrine Society scientific statement. *Endocr Rev* 2009; 30:293–342.
 43. vom Saal FS, Akingbemi BT, Belcher SM, Birnbaum LS, Crain DA, Eriksen M, Farabolini F, Guillette LJ Jr, Hauser R, Heindel JJ, Ho SM, Hunt PA, et al. Chapel Hill bisphenol A expert panel consensus statement: integration of mechanisms, effects in animals and potential to impact human health at current levels of exposure. *Reprod Toxicol* 2007; 24: 131–138.
 44. Anway MD, Cupp AS, Uzumcu M, Skinner MK. Epigenetic transgenerational actions of endocrine disruptors and male fertility. *Science* 2005; 308:1466–1469.
 45. Jirtle RL, Skinner MK. Environmental epigenomics and disease susceptibility. *Nat Rev Genet* 2007; 8:253–262.
 46. Skinner MK, Manikkam M, Guerrero-Bosagna C. Epigenetic transgenerational actions of environmental factors in disease etiology. *Trends Endocrinol Metab* 2010; 21:214–222.
 47. Guerrero-Bosagna C, Settles M, Lucker B, Skinner MK. Epigenetic transgenerational actions of vinclozolin on promoter regions of the sperm epigenome. *PLoS One* 2010; 5:e13100.
 48. Inawaka K, Kawabe M, Takahashi S, Doi Y, Tomigahara Y, Tarui H, Abe J, Kawamura S, Shirai T. Maternal exposure to anti-androgenic compounds, vinclozolin, flutamide and procymidone, has no effects on spermatogenesis and DNA methylation in male rats of subsequent generations. *Toxicol Appl Pharmacol* 2009; 237:178–187.
 49. Schneider S, Kaufmann W, Buesen R, van Ravenzwaay B. Vinclozolin—the lack of a transgenerational effect after oral maternal exposure during organogenesis. *Reprod Toxicol* 2008; 25:352–360.
 50. Ehrlich M, Nelson MR, Stanssens P, Zabeau M, Liloglou T, Xinarianos G, Cantor CR, Field JK, van den Boom D. Quantitative high-throughput analysis of DNA methylation patterns by base-specific cleavage and mass spectrometry. *Proc Natl Acad Sci U S A* 2005; 102:15785–15790.
 51. Deng J, Shoemaker R, Xie B, Gore A, LeProust EM, Antosiewicz-Bourget J, Egli D, Maherali N, Park IH, Yu J, Daley GQ, Eggan K, et al. Targeted bisulfite sequencing reveals changes in DNA methylation associated with nuclear reprogramming. *Nat Biotechnol* 2009; 27:353–360.
 52. Lee EJ, Pei L, Srivastava G, Joshi T, Kushwaha G, Choi JH, Robertson KD, Wang X, Colbourne JK, Zhang L, Schroth GP, Xu D, et al. Targeted bisulfite sequencing by solution hybrid selection and massively parallel sequencing. *Nucleic Acids Res* 2011; 39:e127.
 53. Korshunova Y, Maloney RK, Lakey N, Citek RW, Bacher B, Budiman A, Ordway JM, McCombie WR, Leon J, Jeddeloh JA, McPherson JD. Massively parallel bisulphite pyrosequencing reveals the molecular complexity of breast cancer-associated cytosine-methylation patterns obtained from tissue and serum DNA. *Genome Res* 2008; 18:19–29.
 54. Susiarjo M, Hassold TJ, Freeman E, Hunt PA. Bisphenol A exposure in utero disrupts early oogenesis in the mouse. *PLoS Genet* 2007; 3:e5.
 55. Lawson C, Gieske M, Murdoch B, Ye P, Li Y, Hassold T, Hunt PA. Gene expression in the fetal mouse ovary is altered by exposure to low doses of bisphenol A. *Biol Reprod* 2011; 84:79–86.
 56. Wilks AF, Cozens PJ, Mattaj JW, Jost JP. Estrogen induces a demethylation at the 5' end region of the chicken vitellogenin gene. *Proc Natl Acad Sci U S A* 1982; 79:4252–4255.
 57. Wilks A, Seldran M, Jost JP. An estrogen-dependent demethylation at the 5' end of the chicken vitellogenin gene is independent of DNA synthesis. *Nucleic Acids Res* 1984; 12:1163–1177.
 58. Jost JP, Seldran M, Geiser M. Preferential binding of estrogen-receptor complex to a region containing the estrogen-dependent hypomethylation

- site preceding the chicken vitellogenin II gene. *Proc Natl Acad Sci U S A* 1984; 81:429–433.
59. Kangaspeska S, Stride B, Metivier R, Polycarpou-Schwarz M, Ibberson D, Carmouche RP, Benes V, Gannon F, Reid G. Transient cyclical methylation of promoter DNA. *Nature* 2008; 452:112–115.
 60. Metivier R, Gallais R, Tiffoche C, Le Peron C, Jurkowska RZ, Carmouche RP, Ibberson D, Barath P, Demay F, Reid G, Benes V, Jeltsch A, et al. Cyclical DNA methylation of a transcriptionally active promoter. *Nature* 2008; 452:45–50.
 61. Bretschneider N, Kangaspeska S, Seifert M, Reid G, Gannon F, Denger S. E2-mediated cathepsin D (CTSD) activation involves looping of distal enhancer elements. *Mol Oncol* 2008; 2:182–190.
 62. Branco MR, Ficz G, Reik W. Uncovering the role of 5-hydroxymethylcytosine in the epigenome. *Nat Rev Genet* 2011; 13:7–13.
 63. Bannister SC, Tizard ML, Doran TJ, Sinclair AH, Smith CA. Sexually dimorphic microRNA expression during chicken embryonic gonadal development. *Biol Reprod* 2009; 81:165–176.
 64. Bannister SC, Smith CA, Roeszler KN, Doran TJ, Sinclair AH, Tizard ML. Manipulation of estrogen synthesis alters MIR202* expression in embryonic chicken gonads. *Biol Reprod* 2011; 85:22–30.